Title

A Novel Hypomorphic Apex1 Mouse Model Implicates Apurinic/Apyrimidinic Endonuclease 1 in Oxidative DNA Damage Repair in Gastric Epithelial Cells

Journal

Antioxidants & Redox Signaling, 38(1-3)

ISSN

1523-0864

Authors

Rios-Covian, David

Butcher, Lindsay D

Ablack, Amber L

et al.

Publication Date

2023

DOI

10.1089/ars.2021.0119

Peer reviewed

ANTIOXIDANTS & REDOX SIGNALING
Volume 38, Numbers 1–3, 2023

DOI: 10.1089/ars.2021.0119

ORIGINAL RESEARCH COMMUNICATION

A Novel Hypomorphic *Apex1* Mouse Model Implicates Apurinic/Apyrimidinic Endonuclease 1 in Oxidative DNA Damage Repair in Gastric Epithelial Cells

David Rios-Covian,[1] Lindsay D. Butcher,[2] Amber L. Ablack,[2] Gerco den Hartog,[2] Mason T. Matsubara,[2] Hong Ly,[2] Andrew W. Oates,[1] Guorong Xu,[3] Kathleen M. Fisch,[3] Eric T. Ahrens,[4] Shusuke Toden,[5] Corrie C. Brown,[6] Kenneth Kim,[7] Dzung Le,[1] Lars Eckmann,[2] Bithika Dhar,[8] Tadahide Izumi,[8] Peter B. Ernst,[1,2,9] and Sheila E. Crowe[2]

Abstract

Aims: Though best known for its role in oxidative DNA damage repair, apurinic/apyrimidinic endonuclease 1 (APE1) is a multifunctional protein that regulates multiple host responses during oxidative stress, including the reductive activation of transcription factors. As knockout of the APE1-encoding gene, *Apex1*, is embryonically lethal, we sought to create a viable model with generalized inhibition of APE1 expression.
Results: A hypomorphic (HM) mouse with decreased APE1 expression throughout the body was generated using a construct containing a neomycin resistance (*NeoR*) cassette knocked into the *Apex1* site. Offspring were assessed for APE1 expression, breeding efficiency, and morphology with a focused examination of DNA damage in the stomach. Heterozygotic breeding pairs yielded 50% fewer HM mice than predicted by Mendelian genetics. APE1 expression was reduced up to 90% in the lungs, heart, stomach, and spleen. The HM offspring were typically smaller, and most had a malformed tail. Oxidative DNA damage was increased spontaneously in the stomachs of HM mice. Further, all changes were reversed when the *NeoR* cassette was removed. Primary gastric epithelial cells from HM mice differentiated more quickly and had more evidence of oxidative DNA damage after stimulation with *Helicobacter pylori* or a chemical carcinogen than control lines from wildtype mice.
Innovation: A HM mouse with decreased APE1 expression throughout the body was generated and extensively characterized.
Conclusion: The results suggest that HM mice enable studies of APE1's multiple functions throughout the body. The detailed characterization of the stomach showed that gastric epithelial cells from HM were more susceptible to DNA damage. *Antioxid. Redox Signal.* 38, 183–197.

Keywords: *Apex1*, APE1, oxidative stress, DNA damage, cell differentiation, embryonic development

[1]Center for Veterinary Sciences and Comparative Medicine, Division of Comparative Pathology and Medicine, Department of Pathology, University of California, San Diego, La Jolla, California, USA.
[2]Division of Gastroenterology, Department of Medicine, University of California, San Diego, La Jolla, California, USA.
[3]Center for Computational Biology & Bioinformatics, Department of Medicine, University of California, San Diego, La Jolla, California, USA.
[4]Department of Radiology, University of California, San Diego, La Jolla, California, USA.
[5]Molecular Stethoscope, Inc., San Diego, California, USA.
[6]Department of Pathology, College of Veterinary Medicine, University of Georgia, Athens, Georgia, USA.
[7]La Jolla Institute for Immunology, La Jolla, California, USA.
[8]Department of Toxicology and Cancer Biology, University of Kentucky, Lexington, Kentucky, USA.
[9]Department of Immunology, Chiba University, Chiba, Japan.

Introduction

Apurinic/apyrimidinic endonuclease 1 (APE1, gene name, *Apex1*) is a multifunctional protein that was originally described as a key enzyme mediating repair of abasic DNA lesions induced by oxidative stress (Bhakat et al, 2009; McNeill et al, 2020; Mijit et al, 2021). APE1 also inhibits the accumulation of reactive oxygen species (ROS) (den Hartog et al, 2016), modulates redox-sensitive gene transcription (Bhakat et al, 2009; Bhattacharyya et al, 2009; McNeill et al, 2020; O'Hara et al, 2009; O'Hara et al, 2006; Xanthoudakis et al, 1994), and controls human epithelial responses to different stresses, including bacterial infections, such as *Helicobacter pylori* (den Hartog et al, 2021; Ding et al, 2007; Ding et al, 2004).

APE1 regulates responses to hypoxia (*via* HIF-1α), IL-8 production (*via* NF-κB and AP-1), and apoptosis (*via* caspases-8 and -9, and bax-p53) (Chattopadhyay et al, 2010; Dyballa-Rukes et al, 2017).

Genetic variants of *APEX1* have been described, including some in the carboxy terminus, that impact DNA repair and others in the N-terminus and appear to be associated with an increased risk of intestinal inflammation and oxidative stress (Bardia et al, 2012; Mijit et al, 2021). Polymorphisms in *APEX1*, as well as in other genes of the base excision repair (BER) pathway, such as *MUTYH* and *OGG*, have been associated with an increased risk of developing colorectal cancer (Kasahara et al, 2008; Santos et al, 2014). Thus, APE1 acts as a hub in oxidative stress regulating redox-sensitive responses and oxidative DNA damage.

Animal models are useful for studying human disease. In the case of APE1, the total lack of this protein is embryonically lethal (Ludwig et al, 1998; Meira et al, 2001; Xanthoudakis et al, 1996) due to its crucial role during embryonic development (Xanthoudakis et al, 1996). Models using haplodeficient mice—which typically have a 50% decrease in APE1 expression—have been reported to have no readily identifiable phenotype (Xanthoudakis et al, 1996). Other reports described subtle, organ-specific changes (Raffoul et al, 2004; Unnikrishnan et al, 2009) associated with oxidative stress. Tissue-specific APE1 knockout (KO) mice affect neural genome integrity (Domenis et al, 2014) and the recovery of gray matter after brain stroke (Stetler et al, 2016). Another study using a tamoxifen-inducible whole-body KO showed defects related to growth and development, recovery from wounds, and prevention of senescence (Li et al, 2018).

Hypomorphic (HM) mice are considered an alternative model for studying genes that show a severe phenotype when ablated. Further, they avoid extra interventions, such as tamoxifen administration, and the vagaries associated with the timing of the introduction of the deficiency (Baldini, 2010). The HM mice have been used to gain insights into the mechanisms of action and treatment for several diseases, such as propionic acidemia, dystrophic epidermolysis bullosa, or Huntington's disease (Fritsch et al, 2008; Guenzel et al, 2013; Murthy et al, 2019). The aim of the current study was to develop an HM model to study the consequences of APE1 deficiency from embryonic development to adults with a particular focus on DNA damage in the stomach.

Innovation

Apurinic/apyrimidinic endonuclease 1 (APE1) knockout is embryonically lethal, whereas targeted knockouts usually provide a more limited perspective on APE1 deficiency. We created an APE1 hypomorphic (HM) mouse in which APE1 expression is decreased throughout the body by 80%–90% (Fig. 1) compared with a typical 50% inhibition in heterozygotic mice. The APE1 HM mice revealed subtle effects on fetal survival, growth, and cellular differentiation with a dramatic effect on oxidative DNA damage in the gastric epithelium *in situ* and in primary cell lines. Removal of the neomycin resistance (*NeoR*) cassette restored APE1 expression and reversed all phenotypic changes.

Results

We constructed a conditional knock-out model using the Cre-loxP/Flp-FRT system containing a removable neomycin resistance (*NeoR*) cassette that yielded viable *neo-Apex1*$^{fl/fl}$ mice with limited morphological abnormalities. These mice showed an 80%–90% decrease in APE1 expression in all tissues examined. In addition to impacting fecundity, the attenuated APE1 expression was associated with subtle, isolated changes in differentiation and development but a dramatic increase in oxidative DNA damage in the gastric epithelium (described below). Thus, multiple functions of APE1 are impacted throughout the body when its expression is impaired in this APE1 HM mouse (Fig. 1).

APE1 HM mice embryos are less viable and smaller in size

Mice were created with a construct that included the *NeoR* cassette (Fig. 2A), and the presence of the cassette was confirmed by polymerase chain reaction (PCR) (Fig. 2B). To characterize the model, embryonic health was evaluated by magnetic resonance imaging (MRI) (Supplementary Fig. S1A). The offspring from heterozygotic (Het) parents showed a 50% reduction in the number of HM mice born than would be predicted by Mendelian genetics (Fig. 2C). APE1 expression was assessed by Western blot and found to be markedly lower in the HM fetuses (Supplementary Figs. S1 and S2). Those undergoing resorption had the lowest levels (Supplementary Fig. S1B), suggesting that expression was variable in HM mice and became embryonically lethal when it fell to a critical point.

Genotyping the healthy and resorbing fetuses showed a recovery of the expected Mendelian ratios (data not shown). The role of the *NeoR* cassette in creating the HM phenotype was confirmed by removing the flippase recognition target (FRT)-flanked insert with a backcross to flippase 1 (*Flp1*) mice. This restored the expression of APE1 to normal levels (Fig. 2D, E).

APE1 HM mice have a generalized inhibition of APE1 expression with a few gross aberrations

As this is a novel model for altering APE1 expression, the wildtype (Wt), Het, and HM mice were comprehensively phenotyped. The reduction in APE1 expression correlated to their reduced size (Supplementary Fig. S4A–C Pearson

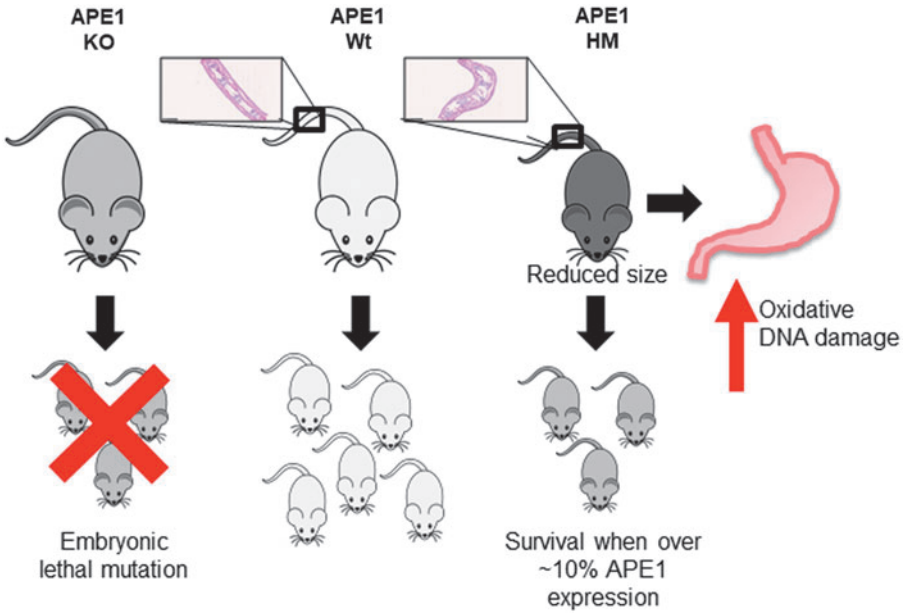

FIG. 1. Multiple functions of APE1 throughout the body. APE1 knockout is embryonically lethal, whereas targeted knockouts usually provide a more limited perspective on APE1 deficiency. We created an APE1 HM mouse in which APE1 expression is decreased throughout the body by 80%–90% compared with a 50% inhibition in Het mice. The APE1 HM mice revealed subtle effects on fetal survival, growth, and cellular differentiation with a dramatic effect on oxidative DNA damage in the gastric epithelium *in situ* and in primary cell lines. Removal of the *NeoR* cassette restored APE1 expression and reversed all phenotypic changes. APE1, apurinic/apyrimidinic endonuclease 1; HM, hypomorphic; *NeoR*, neomycin resistance.

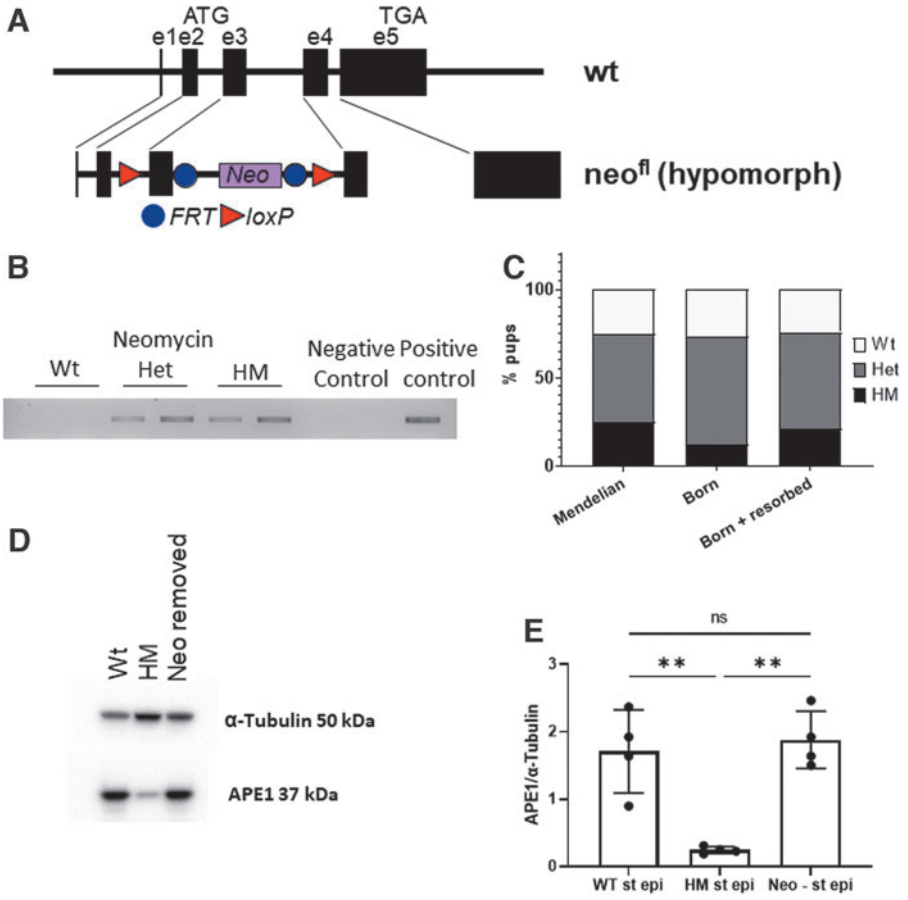

FIG. 2. Establishment of an Apex1 whole-body knockdown mouse model and role of APE1 in embryonic development. **(A)** The whole-body HM genotype was accomplished using a vector containing a neomycin (Neo) cassette flanked by loxP (*red arrowhead*) and FRT (*blue circle*) sites that was located between exons 3 and 4 of the mouse *Apex1* gene. **(B)** The presence of the *NeoR* cassette was confirmed by PCR in the Het and HM mice but was absent in Wt mice. **(C)** The genotype of offspring from Het breeding pairs was not consistent with a Mendelian pattern of inheritance for APE1; however, when resorbed fetuses were considered, Mendelian genotype ratios were essentially restored. **(D)** Western blot for APE1 in isolated gastric epithelial cells (st epi) showed that the presence of the *NeoR* cassette in HM mice impaired APE1 expression, which returned to normal after removing the insert. **(E)** Levels of APE1 expressed in gastric epithelial cells of Wt, HM, and mice with the Neo cassette removed ($n=4$). Neo-, *NeoR* cassette removed. $^{**}p<0.001$ based on one-way ANOVA. ANOVA, analysis of variance; FRT, flippase recognition target; Het, heterozygotic; PCR, polymerase chain reaction; Wt, wildtype.

correlation, $p = 0.0039$). When neonatal or adult mice were assayed by Western blot and immunofluorescence, APE1 was reduced in HM mice (75%–95%) in every tissue examined (Supplementary Figs. S5–S9). Although the Het mice were expected to have intermediate expression, APE1 expression was more variable making comparisons less informative (Supplementary Fig. S5C).

Although there were a few obvious differences among the strains, HM mice usually had malformations of the tail (Supplementary Figs. S3–S5A) and exhibited unusually tough skin with changes in the dermal histology (Supplementary Fig. S5B).

Histological examination of the ileum, colon lungs, liver, spleen, kidney, brain, and heart from HM mice did not reveal any obvious abnormalities even though APE1 expression was reduced in all of these sites (Supplementary Figs. S6–S9). As APE1 has been implicated in regulating innate immunity (Akhter et al, 2016) as well as isotype switch (Frossi et al, 2019), blood work was done to evaluate erythrocytes and leukocytes. No obvious differences were detected (Supplementary Table S2).

Apex1 *function in the stomach*

Previous studies have implicated APE1 in the control of oxidative stress in models of gastric cancer and *H. pylori* infection (Bhandari and Crowe, 2012; Bhattacharyya et al, 2014) so the stomach was studied in detail. As the Wt and HM represented the extremes in APE1 expression, they were the focus for most studies. No differences in gastric morphology were appreciated in HM compared with Wt mice (Fig. 3A). Gastric epithelial cells were enriched for APE1 expression, as they had more intense immunofluorescence than adjacent lamina propria or tunica muscularis tissues (Fig. 3A). Western blot showed that HM mice had an approximate average of 80% reduction in APE1 expression in gastric epithelial cells assayed *in situ* or after isolation (Fig. 3B–D).

Since APE1 plays an essential role in the repair of abasic sites that can progress to single- and double-stranded DNA breaks, DNA damage in the stomach and freshly isolated gastric epithelial cells was assessed with three different approaches. First, we screened for the relative integrity of DNA in freshly isolated gastric epithelial cells from HM or Wt mice by long amplicon (LA)-PCR. As shown in Figure 3E, nuclear DNA integrity was compromised in the epithelium from HM mice compared with Wt. In contrast, leukocyte-enriched populations, from the lamina propria or spleen, lacked detectable loss of DNA integrity (data not shown). Mitochondrial DNA (mtDNA) from gastric epithelial cells prepared from HM mice also had lower DNA integrity when assayed by LA-PCR (Fig. 3F) compared with Wt controls ($p < 0.05$).

To validate the presence of DNA damage observed using the LA-PCR assay, gastric epithelial cells were isolated and assayed by Western blot for phosphorylated H2AX (γH2AX)—a marker of double-stranded DNA break repair that emerges subsequent to the onset of oxidative DNA damage (Murata et al, 2012). As shown in Figure 4, both by Western blot and by flow cytometry, gastric epithelial cells from HM mice had significantly higher levels of γH2AX than Wt cells. To implicate the *NeoR* insert as the reason for the disruption in APE1 expression, its removal (which restored APE1 expression as shown in Fig. 2) prevented the increase in γH2AX, thereby demonstrating that APE1 expression levels were the controlling factor in the accumulated DNA damage found in gastric epithelial cells by the other assays.

Effects of APE1 on gastric epithelial gene expression

APE1 has been implicated in the transcriptional activation regulating the expression for many genes, particularly *in vitro*, including studies of malignant gastric epithelial cells lines (Bhattacharyya et al, 2010; Chattopadhyay et al, 2010; den Hartog et al, 2016; O'Hara et al, 2006). As we sought to develop an *in vitro* system using primary gastric epithelial cells, we first screened the gastric tissue from Wt, Het, and HM mice by RNAseq to determine whether major disruptions could be anticipated. In contrast to many reports studying the role of APE1 in regulating gene expression *in vitro*, relatively few genes were significantly different although *Apex1* was markedly reduced in the HM mice.

Using a 20% false positive rate as a cutoff, a volcano plot showed that the expression of five genes was increased and the remaining that were altered were decreased when messenger RNA (mRNA) from HM and Wt mice were compared (Fig. 5A). Based on an unsupervised hierarchical clustering, 20 differentially expressed genes segregated the three genotypes of mice into different groups (Fig. 5B). Heterozygotic mice showed a gene expression profile more heterogeneous than Wt and HM, but more similar to the Wt.

Using this database, a pathway analysis was performed using Metascape with KEGG, Gene Ontology (GO), and Reactome as outputs (data not shown). The pathways most implicated in HM mice were those related to viral myocarditis, neutrophil-mediated immunity, and purine ribonucleoside metabolism. The downregulated pathways in these mice were collagen fibril organization, amino acid metabolic process and diencephalon development. Previous reports (Domenis et al, 2014; Zou et al, 2007) and the pathway analysis suggested that APE1 may have functions that impact cell division and differentiation in the stomach, so the effect of the loss of APE1 expression on the growth and differentiation of primary gastric epithelial cells was assessed.

Reduced APE1 expression promotes differentiation and early cell death

Primary gastric epithelial cell lines were derived, and proliferation was assessed using the 3-(4,5-dimethylthiazol-2-yl)-2,5-diphenyltetrazolium bromide (MTT) assay. This study revealed a significant difference between Wt and HM cells at 72 h ($p < 0.05$) (Fig. 6A). The survival of HM cells was significantly reduced after 48 h of incubation ($p < 0.05$) compared with Wt cells (Fig. 6B). Selected gene expression was analyzed by quantitative reverse transcriptase-polymerase chain reaction for two stem cell markers (*Lgr5* and *Myc*), two gastric epithelial markers (*Muc5A* and *Tiff1*) as well as *Apex1*. When comparing gene expression in Wt and HM cells, in both undifferentiated and differentiated gastric cell lines (Fig. 6C, D), APE1 levels were lower—as expected—in the HM cells relative to Wt cells ($p < 0.001$). Surprisingly, HM cells had a significantly higher expression of epithelial markers in both undifferentiated and differentiated gastric cell lines, suggesting a role for APE1 in regulating cell differentiation.

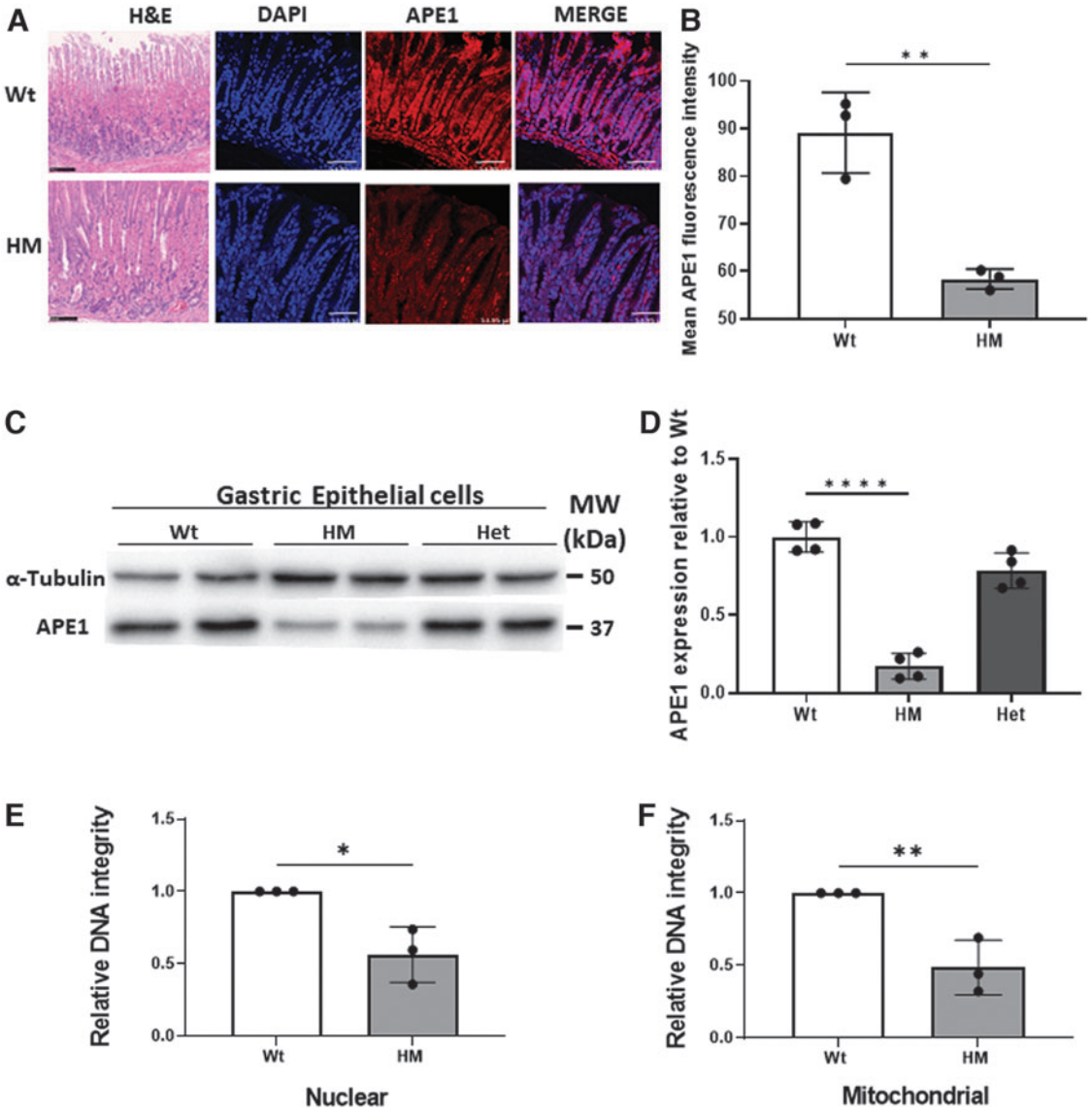

FIG. 3. APE1 is essential for maintaining DNA integrity in the stomach. **(A)** Morphologically, the H&E-stained sections of gastric tissue from Wt and HM appeared indistinguishable (bar = ~50 μm). Immunofluorescent imaging of gastric tissue in HM mice (bar = ~50 μm) showed a virtual lack of APE1 expression compared with Wt mice and counts of positive cells are summarized in **(B)** ($n = 3$). **(C)** Levels of APE1 expressed in gastric epithelial cells measured by Western blot and summarized in **(D)** ($n = 4$). **(E)** DNA damage in freshly isolated gastric epithelial cells was increased when analyzed by LA PCR compared with leukocytes from the lamina propria cells or spleen. Further, examination of DNA integrity by LA PCR in the nucleus or mitochondria of freshly isolated gastric epithelial cells suggested that both organelles were affected **(F)**. $N = 3$. *$p < 0.01$; **$p < 0.001$; ****$p < 0.00001$ **(B, E, F)** based on Student's *t*-test. **(D)** Brown-Forsythe and Welch ANOVA. H&E, hematoxylin and eosin; HM, hypomorphic; LA, long amplicon.

Reduced APE1 expression in primary gastric epithelial cell lines increases DNA damage in response to H. pylori *and methyl methanesulfonate*

The data thus far from comparisons of the HM and Wt mice suggested a role for APE1 in repairing gastric DNA damage. Primary gastric epithelial cells derived from both HM and Wt mice were exposed to two carcinogens: *H. pylori*—which is known to be a trigger for oxidative stress and the major cause of gastric cancer (Bhandari and Crowe, 2012; Bhattacharyya et al, 2014); and methyl methanesulfonate (MMS), which generates AP sites in the genome because methylated purines in DNA are readily depurinated spontaneously (Suganya et al, 2015). The repair of damage induced by MMS thus requires APE1. Moreover, it was reported that alkylated DNA leads to DNA damage and induced increase in intracellular ROS that imparts an oxidative stress capable of causing additional DNA damage, particularly when DNA repair mechanisms are impaired (Rowe et al, 2008).

Primary gastric epithelial cell lines from HM stimulated with *H. pylori* had an increase in 8-hydroxy-2-deoxyguanosine (8-OHdG, a marker of early stages in oxidative DNA damage, Fig. 7A, C) and γH2AX (Fig. 7B, C)

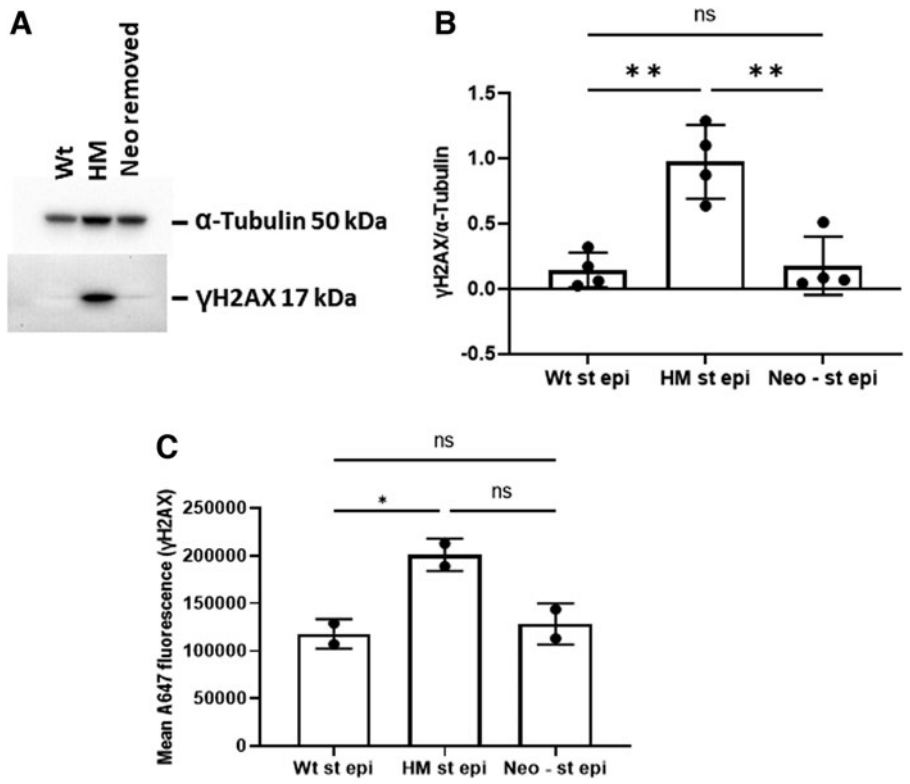

FIG. 4. Removal of the Neo insert prevents increase in DNA damage. (A) Western blot from the same gel as Figure 2 but probed for γH2AX in gastric epithelial cells (st epi) showed that DNA damage returned to background levels with the excision of the *NeoR* insert. **(B)** Summary data of Western blots from **(A)** and validated by flow cytometry for γH2AX **(C)**. $^{*}p < 0.01$; $^{**}p < 0.001$ based on one-way ANOVA. γH2AX, phosphorylated H2AX.

compared with gastric cells from Wt mice. To further implicate the deficiency in APE1 with an increase in DNA damage, cells from HM mice were shown to display an increase in the number of abasic sites ($p < 0.001$, Fig. 7D) and γH2AX ($p < 0.001$, Fig. 7E) *versus* Wt controls after treatment with MMS.

Discussion

This article describes the construction and phenotypic characterization of an APE1 HM mouse. The impaired expression of APE1 was manifest in all tissues examined throughout the body and only partially impacted embryonic viability. Diminished APE1 expression impaired growth, at least early in life, and was associated with a malformation of the tail. Although many tissues lacked any obvious structural defect, the decrease in APE1 expression affected DNA integrity, either constitutively or in substantially increased amounts after exposure to known carcinogens. The role of the *NeoR* cassette in the creation of the HM phenotype was confirmed as any defect in litter size, APE1 expression, tail deformities, and DNA damage disappeared when the insert was removed by back-crossing to *flp* recombinase mice. This backcross, of course, yields floxed APE1 that can be used for developing targeted KO mice. Thus, a novel resource is now available to dissect the role of this multifunctional protein in response to various stresses throughout the body.

APE1 is a multifunctional protein that impacts embryonic lethality, gene transcription, and host responses to oxidative stress. It was first described for its role as an endonuclease repairing abasic sites (Nakabeppu and Sekiguchi, 1981) such as those seen in oxidative DNA damage. Oxidative stress initiates a sequence of events beginning with: accumulation of ROS within the cell; oxidation of bases, particularly guanosine to create 8-OHdG; removal of these bases to yield abasic (apurinic/apyrimidinic) sites; single-strand breaks; and subsequent repair. Alternatively, some single-strand breaks, either by number or by timing, can eventually lead to double-strand breaks and cell death (Murata et al, 2012).

Although a total KO of the *Apex1* gene is embryonically lethal by day 10 (Ludwig et al, 1998; Meira et al, 2001), other approaches have been informative. The most conventional is the use of haplo-insufficient mice (*Apex1*$^{+/-}$) (Meira et al, 2001; Stavnezer et al, 2014; Unnikrishnan et al, 2009; Xanthoudakis et al, 1996); however, the changes in heterozygotic mice with $\sim$50% residual APE1 expression appear modest or variable. Another strategy is the development of a targeted site-specific KO for *Apex1* (Dumitrache et al, 2018; Stetler et al, 2016). Finally, an inducible KO mouse has been developed (Li et al, 2018), showing different phenotypes depending on the age when APE1 elimination was induced. The HM mice have the desired effect of permitting survival of the HM embryos to yield offspring with a lifelong inhibition of APE1 expression throughout the body as seen in other HM models (Baldini, 2010).

The HM mice described here showed a 50% reduction in the expected number of HM mice born. A 10% reduction of expected offspring was reported in *Apex1* haploinsufficient mice (Meira et al, 2001), which suggests that the dose of APE1 affects fecundity. Genotyping of fetuses showed a recovery of Mendelian ratios when the resorbed fetuses were included in the analysis. Monitoring, genotyping, and measurement of APE1 levels in embryos during pregnancy indicated that at least 10%–20% of normal APE1 expression was necessary for survival. APE1 HM mice showed a shorter, curly tail that has not been previously described whereas the size of embryos and neonatal mice was also related to APE1 levels, as mice having less APE1 expression were smaller.

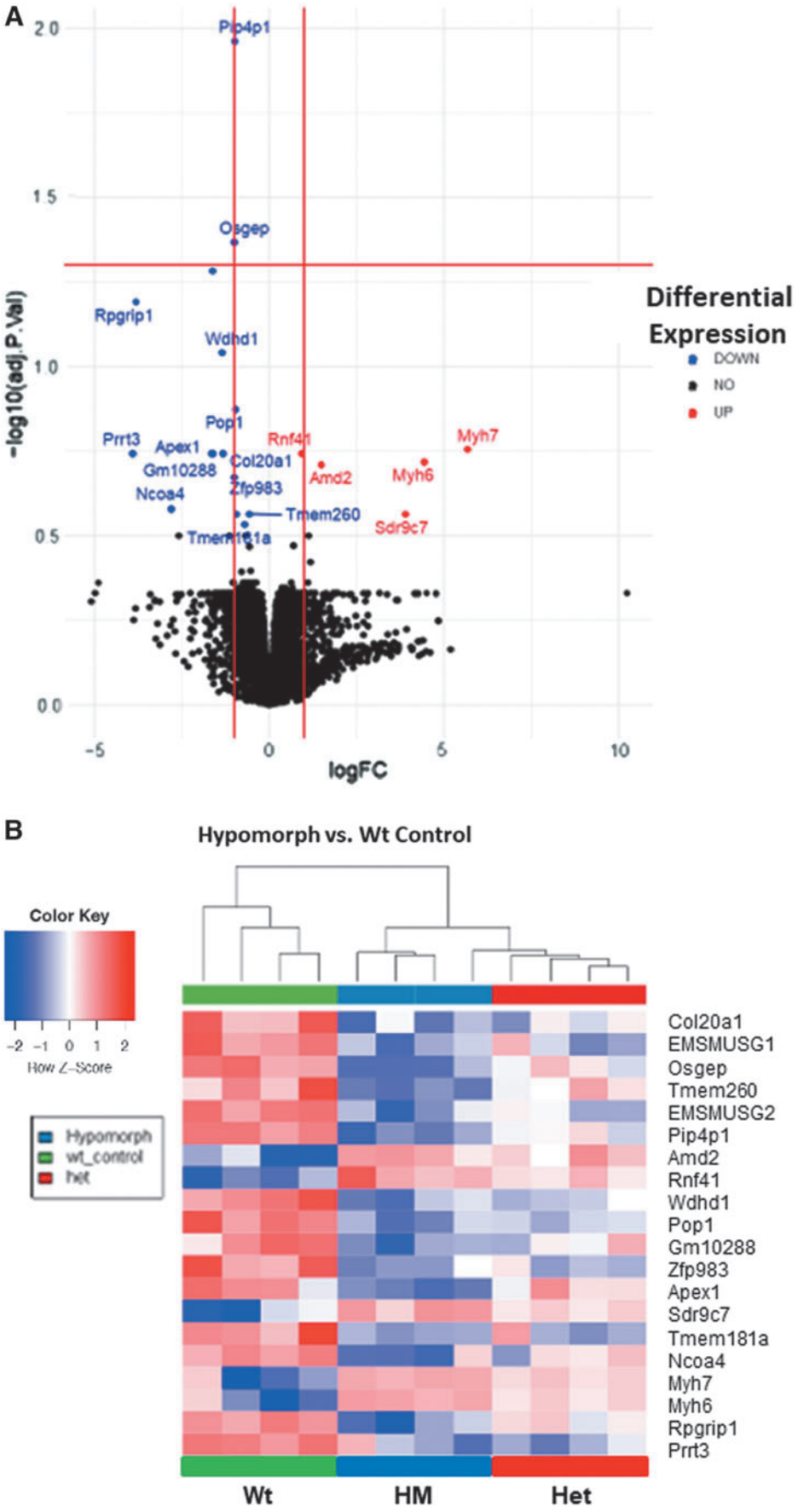

FIG. 5. The effects of APE1 inhibition on gene expression in HM mice. Samples were collected from the gastric mucosa of Wt, Het, or HM mice. mRNA was extracted and analyzed by RNAseq, as described in the methods. Subsequently, data were analyzed using the limma-voom method to identify differentially expressed genes. Using a false positive rate of 20%, the volcano plot highlights marginally significantly differentially expressed genes **(A)**. The heat map summarizes individual-level changes in gene expression among the three strains for the differentially expressed genes (adjusted *p* value <0.2). **(B)** EMSMUSG1 = EMSMUSG00000073455; EMSMUS2 = EMSMUS00000093880. mRNA, messenger RNA.

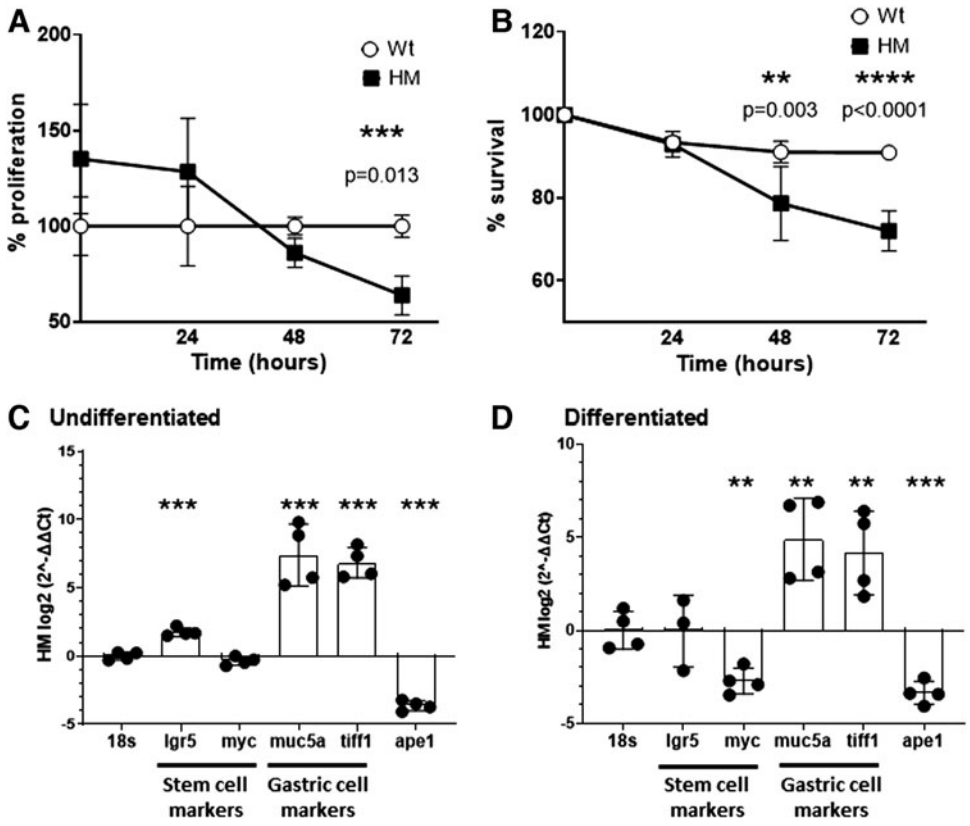

FIG. 6. Primary gastric epithelial cell lines derived from HM mice differentiate prematurely *in vitro* compared with Wt lines. (A) MTT proliferation assay primary gastric epithelial cell lines isolated from Wt and HM mice. **(B)** Survival curve of HM and Wt primary gastric epithelial cell lines measured by trypan blue exclusion. **(C, D)** Fold-change in gene expression in HM relative to Wt shown as log $2^{-\Delta\Delta ct}$ of stem cell marker genes (lgr5 and myc) and gastric differentiation markers (muc5a and tiff1) as well as APE1 in HM cells compared with Wt cells for spheroids **(C)** and differentiated monolayers **(D)** after 24 h of incubation. $n=4$. $^{**}p<0.01$; $^{***}p<0.001$; $^{****}p<0.00001$ based on two-way ANOVA **(A, B)** Student's *t*-test **(C, D)**. HM, hypomorphic; MTT, 3-(4,5-dimethylthiazol-2-yl)-2,5-diphenyltetrazolium bromide.

This phenotype was recapitulated by a tamoxifen-induced APE1 whole-body KO model when tamoxifen was administered at 1 week of age (Li et al, 2018). These authors also reported that when tamoxifen was administered at week 6, size differences were not significant. In our model, as mice get older, the size difference between Wt and HM mice was reduced and was no longer significant after 24 weeks. Thus, APE1 appears to affect growth *in utero* and the neonatal period.

The most extensively studied roles for APE1 are its contributions to the repair of oxidative DNA damage and redox-sensitive gene regulation (Ludwig et al, 1998). The results of RNAseq did not align well with our expectations based on previously published information. Reverse transcriptase-polymerase chain reaction (RT-PCR) was used to validate selected genes, including *Apex1* and *Ncoa4*. Both were reduced in the RNA-seq and RT-PCR assays (data for *Ncoa4* not shown). As the RNAseq data were obtained in gastric mucosal preparations while epithelial cells were the focus of this article, it is possible that the mixing of mRNA from multiple lineages obscures some changes in gene expression. If studies that populated the existing databases relied on cell lines or other tissues, comparisons with a detailed examination of the stomach may be open to misinterpretation.

One of the pathways upregulated in HM mice relates to the myocarditis pathway (data not shown), which has been previously related to differential APE1 expression during inflammation and apoptosis (Ding et al, 2004; Guenzel et al, 2013). It should be noted that when, so few genes are affected in the HM mice, extrapolating the changes in gene expression to pathways was not compelling. Why the myocarditis pathway was altered in the gastric mucosa is unclear but may be biased by the limited databases used in systems biology as well as the role for elements in this molecular network more broadly in inflammation.

Different tissues would have to be compared head-to-head to minimize artefacts attributed to tissue lineage, interexperimental variation, differences in the microbiota, and so on. The lack of agreement with *in vitro* cell systems may also reflect gaps in our knowledge of which genes are expressed in the stomach. In addition, we were not able to manipulate ''dose'' of APE1 *in vivo* in a controlled manner, so some of the changes may reflect a partial knockdown and not the results of the total removal of APE1. Further, this is not the first time that *in vitro* functions of APE1 were not recapitulated in an animal model. For example, a cysteine residue in the amino terminus was shown to be reduced and instrumental in the reductive activation of transcription factors *in vitro* (Xanthoudakis et al, 1994).

However, when this residue was mutated and knocked into mice, no difference in the activation of the studied transcription factors or gene expression was found (Ordway et al, 2003). It should be noted that other studies do not find that this residue is completely benign (Vascotto et al, 2011). This points to the unknown interactions and potential redundancies that exist in nature to protect against loss of function mutations in important molecules. As *Apex1* was reduced in the RNAseq and epithelial cell studies, this article focused on the results for *Apex1* in the HM mice.

A constitutive increase in DNA damage in the HM mice detected by multiple, biologically independent assays was a very reproducible observation that fits in with the known functions of APE1. Further, *H. pylori*, a known carcinogen

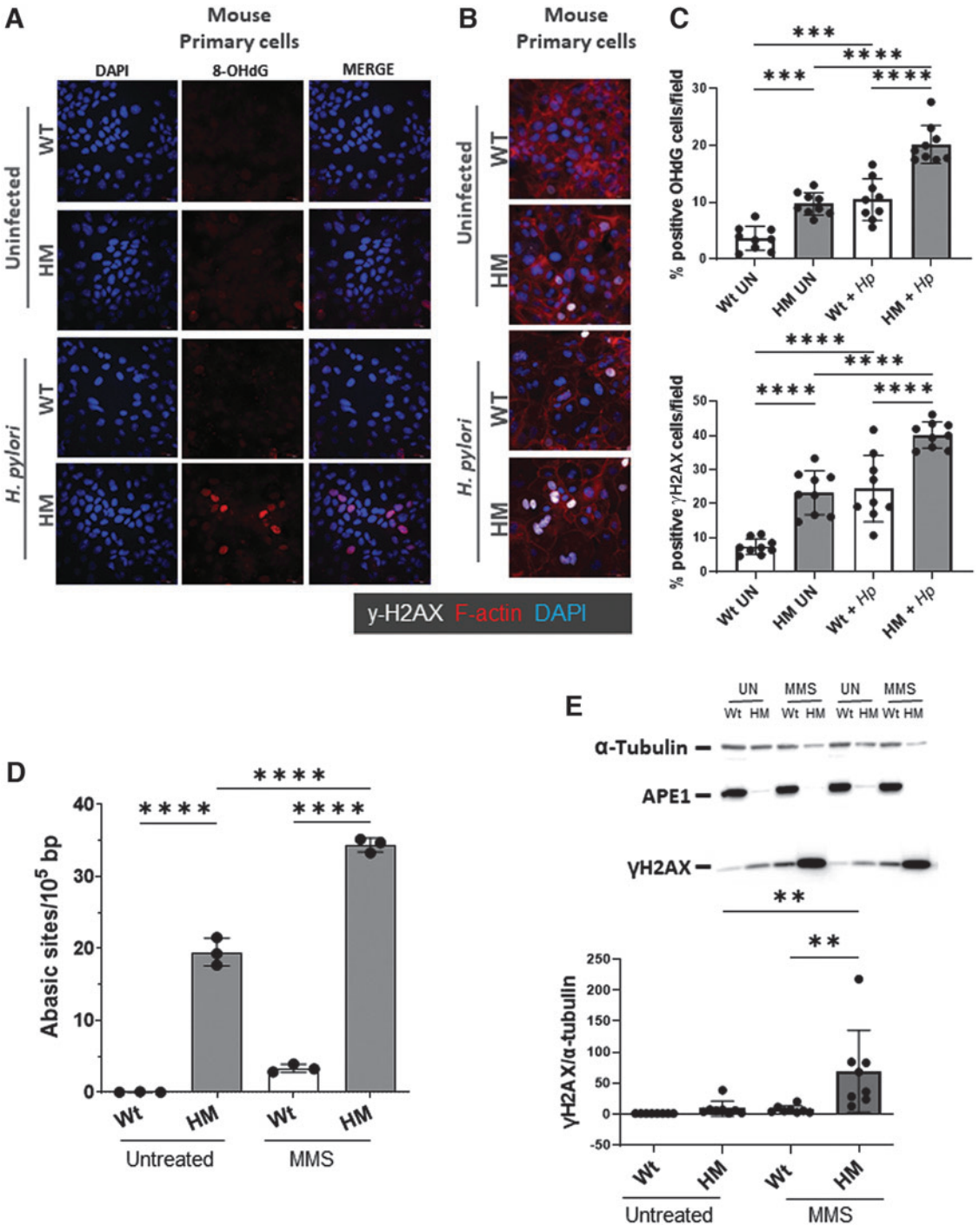

FIG. 7. Reduced APE1 expression increases oxidative DNA damage in response to *Helicobacter pylori* and MMS. Primary gastric epithelial cell lines from HM or Wt mice were stimulated with *H. pylori* at MOI 100. Subsequently, cells were assayed for 8-OH guanosine **(A)** or γH2AX **(B)**. 8-OH guanosine was increased in primary mouse GECs from HM mice relative to Wt following *H. pylori* infection **(A)**. Confocal analysis of mouse gastric epithelial cells for γH2AX following infection with *H. pylori* at MOI 100 for 24 hours **(B)**. *Red* F-actin, *White* γH2AX, *blue* DAPI. Graphs summarizing panels A and B are shown in **C**. To compare responses to another known carcinogen, primary mouse GEC were exposed to MMS and assayed for the presence of abasic sites **(D)** or γH2AX **(E)** ($n=3$). Both *H. pylori* and MMS increased changes in DNA that are associated with oxidative stress. *$p<0.05$; ***$p<0.0001$; ****$p<0.00001$. GEC, gastric epithelial cells; HM, hypomorphic; MOI, multiplicity of infection; Wt, Wildtype.

that leads to gastric cancer (Forman, 1996), was shown to be sufficient to increase the accumulation of ROS and oxidative DNA damage in gastric epithelial cells (Baik et al, 1996). The data in this study document the signature change in oxidative DNA damage, an increase in 8-OH2dG, which was then followed by an increase in γH2AX. As previously reported (Suganya et al, 2015), MMS can induce an increase in AP sites DNA in cells deficient in APE1.

The results reported here would agree with a previous report implicating MMS in the induction of a secondary

oxidative stress after DNA damage induced by the alkylation of DNA (Rowe et al, 2008). DNA damage induced by exposure to ultraviolet light or MMS was followed by an increase in oxidative stress and molecular changes that would reflect secondary oxidative DNA damage (Rowe et al, 2008). Thus, our observations are consistent with the notion that MMS induces a secondary oxidative DNA damage that is increased when APE1 expression is reduced.

APE1 has been related to the lack of hair and slower hair growth in a tamoxifen-induced KO model (Li et al, 2018). In HM mice, this phenotype was not recapitulated, possibly because HM skin still has at least 10% of normal APE1 expression, which may be sufficient to prevent the phenotype. Other studies have implicated APE1 in skin health, as the overexpression of this gene occurs in the dermis of psoriatic patients compared with healthy subjects (Lee et al, 2009). The skin from HM mice was very resilient and had morphological changes to suggest that APE1 regulates cells in this site as well.

The current study showed that APE1 expression is higher in undifferentiated Wt gastric epithelial cells than in HM cells. Surprisingly, the intestinal differentiation markers *Muc5a* and *Tiff1* were highly expressed in HM cells in both spheroids and monolayers compared with Wt cells. RNA expression analysis for genes associated with differentiation suggested a dysregulation in HM cells, although the study was underpowered to fully describe the changes. The mechanistic insight and the pathways implicated in this phenomenon require further investigation.

Conclusion

In conclusion, this novel HM model provides a lifelong disruption in APE1 expression/function that might be useful as a model for loss-of-function polymorphisms in human *APEX1* that impact the multiple roles of this molecule in homeostasis and oxidative stress, including those associated with a higher risk of cancer development (Lirussi et al, 2016).

Materials and Methods

Generation of the construct

Apex1 KO mice are embryonically lethal, so a construct was designed to create an inducible KO mouse that contained a *NeoR* selection cassette (Fig. 2A). The construct was designed so the *NeoR* cassette was inserted between the third and fourth exon so that it might create an HM mouse. This site was flanked by FRT sites so the cassette could be removed by breeding to an Flp recombinase-expressing mouse. The third exon was flanked by two loxP sites, enabling it to be removed by crossing to mice expressing Cre. The presence of the *NeoR* cassette was confirmed using the primers F-GTCTTGTCGATCAGGATGATCTGG and R-ACTCGTCAAGAAGGCGATAGAAGG.

Mice

All procedures were reviewed and approved by the UCSD Animal Care and Utilization Committee (S00205 or S11169). Mice were generated using embryonic stem cells (origin strain 129X1/SvJ x 129S1) to yield a strain registered as B6N;129-*Apex1*^{tm1Ernst}/Mmucd mice. This strain was donated to the Mutant Mouse Regional Resource Center at University of California, Davis for cryo-archiving and distribution under stock number 041844-UCD (repository grant U42 OD012210). Histology slides, blocks, and biobanked tissues can be obtained from the communicating author.

Male and female mice heterozygotic for the Neo construct (*neo-Apex1*$^{fl/+}$) were bred to yield wildtype (*Apex1*$^{+/+}$), heterozygotic (*neo-Apex1*$^{fl/+}$), and the homozygous (*neo-Apex1*$^{fl/fl}$) hypomorphic mice (referred to, respectively, as Wt, Het, and HM hereafter). All mice were genotyped using the primers *Apex1*-loxF (GGCAAGTTCAGGGCTTTAC TAGACC) and *Apex1*-loxR (GTAGTAAGAGCTGGCAG TTCCAACC). Records were collected for all breeding pairs and offspring and phenotyped for body weight and other traits. For tissue harvest, mice were anesthetized with isofluorane and bled. Subsequently, the sedated animals were euthanized by cervical dislocation and tissues were collected for the various procedures.

The *NeoR* insert in the vector used to genetically modify the mice was flanked with FRT sites so that when mice were bred to *Flp1* mice, the *NeoR* insert was excised to yield offspring with a floxed *Apex1* gene but no other changes. The impact of the insert was determined by comparing APE1 expression and function in the offspring, as described next.

Western blot

For Western blot analyses, cells or tissues from 9- to 12-week-old mice were washed twice with ice-cold phosphate buffered saline (PBS) and lysed in RIPA buffer containing protease (Sigma) and phosphatase inhibitors (Thermo Scientific) for 10 min on ice. Lysates were centrifuged for 10 min at 10,000 *g* at 4°C and supernatants were used for quantification of protein levels using the Bradford assay. Fifty micrograms of protein were used per sample, and Laemli buffer with ß-mercaptoethanol was added before being boiled for 5 min.

Antibodies used for Western blot were: mouse monoclonal anti-APE1 13B8E5C2 (Novus Biologicals), mouse monoclonal anti-α-Tubulin clone DM1A (Abcam), mouse monoclonal and rat anti-γH2AX (BioLegend). The anti-APE1 antibody was chosen, as it recognizes an epitope between AA 80–100 that is outside of the loxp sites that bracket the insert. This antibody can detect APE1 comparably in Wt and floxed APE1 (after *NeoR* insert is removed), which suggests that the construct did not obscure protein detection. The APE1 and γH2AX mouse monoclonal Abs were used at 1:1000, and α-Tubulin served as a loading control. The secondary antibodies were anti-rabbit or anti-mouse HRP-conjugated IgG (Cell Signaling Technology) using the manufacturer's instructions. Expression was analyzed by densitometry with Image J software (Schneider et al, 2012).

Blood work

Blood was collected by cardiac puncture and collected in EDTA-containing polypropylene microtubes (Microtainer Tubes; Cat. No. 365973; Becton Dickinson). Samples were then analyzed by the UCSD Murine Hematology and Coagulation Laboratory for analysis.

Imaging

Radiographs were obtained by the UCSD Animal Care Program. Three-dimensional, *in vivo* MRI anatomical scans

were obtained for Wt, Het, and HM mice (8–12 weeks of age). In some cases, anesthetized pregnant dams (days 18–21) were used to evaluate fetal loss by MRI. Scans were performed using a Bruker BioSpec 11.7 T MRI system at the Molecular Imaging Center at Sanford Consortium for Regenerative Medicine and using ParaVision 6 software and a 38 mm 1H volume coil (Bruker BioSpin, Billerica, MA).

Mice were anesthetized using 1%–2% isoflurane in oxygen, and body temperature was maintained throughout the procedure using heated air. Anatomical 1H scans in the abdominal region were acquired using a RARE (rapid acquisition with relaxation enhancement) pulse sequence with acquisition parameters: RARE factor 8, repetition time = 1932 ms, echo time = 26.3 ms, field of view = 30×50, matrix size = 156×256, in-plane resolution = $0.192 \times 0.195\ mm^2$, coronal slice orientation, 0.75 mm slice thickness, and 32 slices.

Fetus analysis

Pregnant dams were euthanized based on their MRI images. Uteri were dissected, fetuses were removed, and crown-rump lengths were measured. Fetuses were sectioned longitudinally, using one half for histopathology and the other half for genotyping and Western blot analyses.

Histology and immunofluorescence

Tissues fixed for 24 h in 10% zinc formalin were transferred to 70% ethanol, paraffin-embedded, sectioned, and stained with hematoxylin and eosin. Unstained sections were used for antibody staining. Slides were incubated overnight at 4°C with APE1 antibody, then washed three times for 10 min with PBS +0.0001% triton X-100, and finally incubated for 1 h at room temperature with Alexa-568 conjugated goat anti-mouse antibody (Life Technologies). Slides were washed before Hoechst 33258 dye was added in PBS (1:2000) and incubated for 10 min.

The slides were washed three times for 5 min in PBS, mounted in Prolong Diamond, and imaged using a Leica SP8 confocal microscope. Images were acquired with LAS X software. Additional analysis was performed with ImageJ. hematoxylin and eosin-stained sections were scanned with a Hamamatsu Nanozoomer 2.0HT Slide Scanner at the UCSD microscopy core using brightfield and fluorescence as indicated. The sections were viewed using NDP viewer.

Mouse primary gastric epithelial cells

Freshly isolated epithelial cells were collected from the mouse stomach and studied directly or used to generate undifferentiated or differentiated primary gastric epithelial cells lines as previously described (Miyoshi and Stappenbeck, 2013). Briefly, tissue samples were cut into small pieces and digested with collagenase (Life Technologies) at 37°C for 30 min to 1 h. Cells were then washed with Dulbecco's MEM (Sigma) and filtered. Cultures were maintained in medium containing Wnt3a, R-spondin, and Noggin in Matrigel (Corning).

Media change or cell passage was done every other day. For cell differentiation assays, monolayers were grown on plastic surfaces pretreated with a 1:30 diluted Matrigel solution for 20 min and removed before plating. Cells were incubated with differentiation media that was refreshed each day.

Proliferation of the primary gastric epithelial cell lines was measured using a modified MTT assay (Grabinger et al, 2014). Briefly, 10^5 cells were incubated in matrigel for each condition. At 24, 48, and 72 h, 200 μL of medium with MTT at 500 μg/mL was added to each well for 3 h at 37°C in 5% CO_2. The MTT medium was aspirated and replaced by 2% SDS, and it was then incubated for 2 h at 37°C. Finally, DMSO was added for 1 h at 37°C. After incubation, absorbance was measured at 562nm. To assess survival, primary, undifferentiated gastric epithelial cell lines from Wt and HM were grown as previously described (Grabinger et al, 2014) with 50% conditioned medium for 72 h changing media every 24 h. Cells were detached from the plate, Matrigel was dissolved with trypsin (Sigma), and cells were stained with Trypan blue and counted.

Long amplicon-PCR

LA-PCR assay was carried out as previously described (50). Genomic DNA extraction was done using the Gentra Puregene Kit (Qiagen) with the manufacturer's directions. After quantitation by Pico Green (Molecular Probes) in a 96-well plate and NanoDrop, gene-specific long amplicon-PCR (LA-PCR) analysis for measuring DNA damage was performed using LongAmp Taq DNA polymerase (New England Biolabs). LA-PCR was carried out to amplify a 6.5 kb region around the mouse *PolB* in mouse genomic DNA. The following primers were used for nuclear DNA: 5′-TATC TCTCTTCCTCTTCACTTCTCCCC-3′ (MBFor1) and 5′-CGTGATGCCGCCGTTGAGGGTCTCC-3′ (MBEX1B) for amplifying a region in the *PolB* (Santos et al, 2014). For mtDNA, oligos (5′-AAAACTAGGCCTCGCCCCATTCCAC-3′) and (5′-GGAGTGATGATGTGAGGCCATGTGCGA-3′) were used.

The final PCR reaction condition was standardized at 94°C-30 s; (94°C-30 s, 63°C-30 s, 65°C-10 min) for 25 cycles; 65°C-10 min 15 ng of DNA template was used in each case. A small DNA fragment for each was also amplified to normalize amplification of large fragments using the following primers: 5′-TATGGACCCCCATGAGGAACA-3′ and 5′-AACCGTCGGCTAAAGACGTG-3′ for nuclear DNA, and 5′-GCATACCCCTTCATCCTTCTCTCCC-3′ and 5′-GATGATGTGAGGCCATGTGCG-3′ for mtDNA. The PCR reaction condition was 94°C-30 s; (94°C-30 s, 60°C-20 s, 65°C-30 s) for 25 cycles. Amplified products were visualized on gels and quantified with ImageJ automated digitizing system (NIH).

Bacteria

H. pylori strain SS1 was used as previously described (Alam et al, 2009; O'Hara et al, 2006) and used to infect the primary gastric epithelial cell lines. *H. pylori* organisms were maintained on blood agar plates at 37°C and 10% CO_2 and passaged every 2 or 3 days. For experiments, *H. pylori* was grown in Brucella broth supplemented with 10% fetal bovine serum and grown at 37°C and 10% CO_2 with rocking until an optical density (OD_{600}) of 0.8 was reached.

Oxidative DNA damage

Primary gastric epithelial cells grown from Wt and HM mice were differentiated overnight on collagen IV (Sigma) coated glass chamber slides in 5% CM. Cells were infected at

a multiplicity of infection of 100 with *H. pylori* SS1 for 24 h and then washed and fixed with 2% formaldehyde for 15 min. Slides were washed and permeabilized with 0.2% triton X-100 and subjected to 1 h of blocking solution (1.5% bovine serum albumin [BSA], 5% goat serum in PBS with 0.2% triton X-100). The slides were stained with 8-OHdG (ab48508; Abcam) or γH2AX (613402; BioLegend) antibodies diluted 1:200 in blocking buffer for 2 h at room temperature. Alexa-conjugated secondary antibodies (Life Technologies) were used at 1:400 and incubated for 1 h at room temperature.

Slides were washed before Phalloidin (1:200) was added in 1% BSA for 15 min. After washing, Hoechst 33258 dye in PBS (1:2000) was added and incubated for 10 min. The slides were washed three times for 5 min in PBS, mounted in Prolong Diamond, and imaged using a Leica SP8 confocal microscope. Images were acquired with LAS X software. Additional analysis was performed with ImageJ.

Apurinic/apyrimidinic base assay

DNA was extracted using the PureGene kit (Qiagen) following the manufacturer's instructions. Cells were labeled with HRP using the Dojindo apurinic/apyrimidinic base assay (AP assay) kit. HRP-labeled DNA was quantified using a NanoDrop, and concentration was adjusted to 2.5 ng/μL in every sample before assaying. DNA was then attached to a 96-well plate and washed before releasing the HRP enzyme. The plate was read on a SpectraMax at 650 nm, and the number of abasic sites was determined from the assay standards.

Quantitative real-time PCR

Primary analysis was performed using the pipeline tool Cirrus-NGS (https://github.com/ucsd-ccbb/cirrus-ngs) detailed as follows. RNA was extracted using the mRNA easy kit (Qiagen) according to the manufacturer's instructions. Fifty microliters of RNA was used for obtaining complementary DNA (cDNA) using qScript kit (Quantabio). qPCR was performed with SYBR green (BioTool) in a StepOnePlus System real-time PCR system (Applied Biosystems). Primers used are listed in Supplementary Table S1. Results were analyzed and presented as fold-change expression using the log $2^{-\Delta\Delta ct}$ (Livak and Schmittgen, 2001).

RNA-Seq analysis

Stomach tissues from four mice for the Wt, Het, and HM mice were used as a source of RNA that was extracted using the PureLink RNA preparation kit (Fisher Scientific). RNA samples were checked for their quality using a bioanalyzer (Agilent) and examined for whole transcriptome sequencing (RNA-seq) at the Oncogenomics Core facility of the University of Kentucky. RNA-Seq libraries were prepared using KAPA RNA Hyper+RiboErase HMR (Roche). The manufacturer's protocols were used to sequence ribosomal RNA-depleted libraries at 1×100 single-end read on an Illumina HiSeq 2500 in rapid mode, to an average depth of (40×10^6) paired-end reads per sample.

The data were stored as FASTQ files. Quality control of the raw FASTQ files was performed using the software tool FastQC (De Sena Brandine and Smith, 2019). Subsequently, data were analyzed using the limma-voom method to identify differentially expressed genes. Sequencing reads were aligned to the mouse genome (mm10) using the STAR v2.5.3a aligner (Dobin et al, 2013). Read quantification was performed with RSEM3 v1.3.0 and GENCODE annotation (Mus_musculus.GRCm38
.68.gtf). The R BioConductor packages edgeR (Robinson et al, 2010) and limma (Ritchie et al, 2015) were used to implement the limma-voom (Law et al, 2014) method for differential expression analysis.

Low expressed genes were filtered out (cpm >1 in at least one sample). Trimmed mean of M-values (TMM) (Subramanian et al, 2005) normalization was applied. The experimental design was modeled upon condition and treatment (~ 0 + condition treatment). Significance was defined by using an adjusted p-value cut-off of 0.05 after multiple testing correction using a moderated t-statistic in Limma and a relaxed threshold. Using a false positive rate of 20%, volcano plots were created to reveal marginally significant differentially expressed genes. Pathway analysis was conducted using Metascape (Zhou et al, 2019), using databases for KEGG pathway (hsa), GO, and Reactome (R-HSA). We input marginally differentially expressed genes (raw $p < 0.05$ and fold change $> \pm 1.5$), setting *Mus musculus* as the input species and *Homo sapiens* as the analysis species in Metascape. Identified pathways were ranked based on the p-values, with Metascape multiple comparisons correction applied.

General statistical methods/analysis

Graphpad 9 software was used to plot and perform statistical analysis and reported as the mean ± standard deviation. Analysis of variance and Student t-tests were used according to the data characteristics.

Acknowledgments

The authors would like to acknowledge the technical support received from Lucia Hall and Elaine Hansen. The preparation of sections for histology was done by the Histology Core at the La Jolla Institute for Immunology.

Authors' Contributions

L.D.B., G.H., P.B.E., and S.E.C. conceived the project and the original idea. L.D.B., A.L.A., G.H., M.T.M., H.L., A.W.O., and D.R.-C. performed many of the experiments. T.I., G.X., K.M.F., and S.T. performed the RNAseq analysis. T.I., L.E., D.L., and P.B.E. conceived and developed the mice line. P.B.E., C.C.B., K.K., and D.R.-C. performed the histological assessments. E.T.A. performed the MRI imaging. D.R.-C. and P.B.E. wrote the final version of the article. All authors supervised and approved the final version of the article.

Author Disclosure Statement

The authors have no conflicts of interest related to the current studies. None of the data have been previously published but have been presented in part at national meetings.

Funding Information

Research reported in this publication was supported by the National Institutes of Health under Awards: R01-AI079145, P30-DK120515 and UL-1TR001442, T35-OD010956,

R03CA249111 as well as the Chiba University-UC San Diego Center for Mucosal Immunology, Allergy and Vaccine Development. This research was also supported by the Shared Resource Facilities of the University of Kentucky Markey Cancer Center (P30CA177558). The microscopy facility was supported by the UCSD Cancer Center Specialized Support Grant P30 CA23100 and NS047101. The authors are grateful for the technical support, products, and/or services provided to their research by the Mouse Biology Program (MBP) at the University of California Davis funded by U42OD012210 and the Animal Care Program at UCSD.

Supplementary Material

Supplementary Table S1
Supplementary Table S2
Supplementary Figure S1
Supplementary Figure S2
Supplementary Figure S3
Supplementary Figure S4
Supplementary Figure S5
Supplementary Figure S6
Supplementary Figure S7
Supplementary Figure S8
Supplementary Figure S9

References

Akhter N, Takeda Y, Nara H, et al. Apurinic/apyrimidinic endonuclease 1/redox factor-1 (Ape1/Ref-1) modulates antigen presenting cell-mediated T helper cell type 1 responses. J Biol Chem 2016;291(45):23672–23680; doi: 10.1074/jbc.M116.742353

Alam MS, Kurtz CC, Wilson JM, et al. A2A adenosine receptor (AR) activation inhibits pro-inflammatory cytokine production by human $CD4^+$ helper T cells and regulates Helicobacter-induced gastritis and bacterial persistence. Mucosal Immunol 2009;2(3):232–242; doi: 10.1086/596205.

Baik SC, Youn HS, Chung MH, et al. Increased oxidative DNA damage in *Helicobacter pylori*-infected human gastric mucosa. Cancer Res 1996;56(6):1279–1282.

Baldini A. Mouse as a Model for Human Disease. In: Vogel and Motulsky's Human Genetics. (Speicher MR, Motulsky AG, Antonarakis SE. eds.) Springer: Berlin, Heidelberg, 2010; pp. 779–785.

Bardia A, Tiwari SK, Gunisetty S, et al. Functional polymorphisms in XRCC-1 and APE-1 contribute to increased apoptosis and risk of ulcerative colitis. Inflamm Res 2012;61(4):359–365; doi: 10.1007/s00011-011-0418-2

Bhakat KK, Mantha AK, Mitra S. Transcriptional regulatory functions of mammalian AP-endonuclease (APE1/Ref-1), an essential multifunctional protein. Antioxid Redox Signal 2009;11(3):621–638; doi: 10.1089/ars.2008.2198.

Bhandari A, Crowe SE. *Helicobacter pylori* in gastric malignancies. Curr Gastroenterol Rep 2012;14(6):489–496; doi: 10.1007/s11894-012-0296-y

Bhattacharyya A, Chattopadhyay R, Burnette BR, et al. Acetylation of apurinic/apyrimidinic endonuclease-1 regulates *Helicobacter pylori*-mediated gastric epithelial cell apoptosis. Gastroenterology 2009;136(7):2258–2269; doi: 10.1053/j.gastro.2009.02.014

Bhattacharyya A, Chattopadhyay R, Hall EH, et al. Mechanism of hypoxia-inducible factor 1 alpha-mediated Mcl1 regulation in *Helicobacter pylori*-infected human gastric epithelium. Am J Physiol Gastrointest Liver Physiol 2010;299(5):G1177–G1186; doi: 10.1152/ajpgi.00372.2010

Bhattacharyya A, Mitra S. Chattopadhyay R, et al. Oxidative stress: Role in the pathogenesis of gastrointestinal mucosal diseases. Physiol Rev 2014;94(2):329–354; doi: 10.1152/physrev.00040.2012.

Chattopadhyay R, Bhattacharyya A, Crowe SE. Dual regulation by apurinic/apyrimidinic endonuclease-1 inhibits gastric epithelial cell apoptosis during *Helicobacter pylori* infection. Cancer Res 2010;70(7):2799–2808; doi: 10.1371/journal.ppat.1005382

den Hartog G, Butcher LD, Ablack AL, et al. Apurinic/apyrimidinic endonuclease 1 restricts the internalization of bacteria into human intestinal epithelial cells through the inhibition of Rac1. Front Immunol 2021;11:553994; doi: 10.3389/fimmu.2020.553994

den Hartog G, Chattopadhyay R, Ablack A, et al. Regulation of Rac1 and reactive oxygen species production in response to infection of gastrointestinal epithelia. PLoS Pathog 2016;12(1):e1005382; doi: 10.1371/journal.ppat.1005382

De Sena Brandine G, Smith AD. Falco: high-speed FastQC emulation for quality control of sequencing data. F1000 Research 2019;8:1874–1881; doi: 10.12688/f1000research.21142.2

Ding SZ, Minohara Y, Fan XJ, et al. *Helicobacter pylori* infection induces oxidative stress and programmed cell death in human gastric epithelial cells. Infect Immun 2007;75(8):4030–4039; doi: 10.1128/IAI.00172-07.

Ding S-Z, O'Hara AM, Denning TL, et al. *Helicobacter pylori* and H_2O_2 increase AP endonuclease-1/redox factor-1 expression in human gastric epithelial cells. Gastroenterology 2004;127(3):845–858; doi: 10.1053/j.gastro.2004.06.017

Dobin A, Davis CA, Schlesinger F, et al. STAR: Ultrafast universal RNA-seq aligner. Bioinformatics 2013;29(1):15–21; doi: 10.1093/bioinformatics/bts635

Domenis R, Bergamin N, Gianfranceschi G, et al. The redox function of APE1 is involved in the differentiation process of stem cells toward a neuronal cell fate. PLoS One 2014;9(2):e89232; doi: 10.1371/journal.pone.0089232

Dumitrache LC, Shimada M, Downing SM, et al. Apurinic endonuclease-1 preserves neural genome integrity to maintain homeostasis and thermoregulation and prevent brain tumors. Proc Natl Acad Sci U S A 2018;115(52):E12285–E12294; doi: 10.1073/pnas.1809682115

Dyballa-Rukes N, Jakobs P, Eckers A, et al. The anti-apoptotic properties of APEX1 in the endothelium require the first 20 amino acids and converge on thioredoxin-1. Antioxid Redox Signal 2017;26(12):616–629; doi: 10.1089/ars.2016.6799

Forman D. *Helicobacter pylori* and gastric cancer. Scand J Gastroenterol Suppl 1996;220:23–26.

Fritsch A, Loeckermann S, Kern JS, et al. A hypomorphic mouse model of dystrophic epidermolysis bullosa reveals mechanisms of disease and response to fibroblast therapy. J Clin Invest 2008;118(5):1669–1679; doi: 10.1172/JCI34292

Frossi B, Antoniali G, Yu K, et al. Endonuclease and redox activities of human apurinic/apyrimidinic endonuclease 1 have distinctive and essential functions in IgA class switch recombination. J Biol Chem 2019;294(13):5198–5207; doi: 10.1074/jbc.RA118.006601

Grabinger T, Luks L, Kostadinova F, et al. Ex vivo culture of intestinal crypt organoids as a model system for assessing cell death induction in intestinal epithelial cells and enteropathy. Cell Death Dis 2014;5:e1228; doi: 10.1038/cddis.2014.183

Guenzel AJ, Hofherr SE, Hillestad M, et al. Generation of a hypomorphic model of propionic acidemia amenable to gene therapy testing. Mol Ther 2013;21(7):1316–1323; doi: 10.1038/mt.2013.68

Kasahara M, Osawa K, Yoshida K, et al. Association of MUTYH Gln324His and APEX1 Asp148Glu with colorectal cancer and smoking in a Japanese population. J Exp Clin Cancer Res 2008;27(1):49; doi: 10.1186/1756-9966-27-49

Law CW, Chen Y, Shi W, et al. voom: Precision weights unlock linear model analysis tools for RNA-seq read counts. Genome Biol 2014;15(2):R29; doi: 10.1186/gb-2014-15-2-r29

Lee H-M, Yuk J-M, Shin D-M, et al. Apurinic/apyrimidinic endonuclease 1 is a key modulator of keratinocyte inflammatory responses. J Immunol 2009;183(10):6839–6848; doi: 10.4049/jimmunol.0901856

Li M, Yang X, Lu X, et al. APE1 deficiency promotes cellular senescence and premature aging features. Nucleic Acid Res 2018;46(11):5664–5677; doi: 10.1093/nar/gky326

Lirussi L, Antoniali G, D'Ambrosio C, et al. APE1 polymorphic variants cause persistent genomic stress and affect cancer cell proliferation. Oncotarget 2016;7(18):26293–26306; doi: 10.18632/oncotarget.8477

Livak KJ, Schmittgen TD. Analysis of relative gene expression data using real-time quantitative PCR and the 2(-delta delta C(T)) method. Methods 2001;25(4):402–408; doi: 10.1006/meth.2001.1262.

Ludwig DL, Macinnes MA, Takiguchi Y, et al. A murine AP-endonuclease gene-targeted deficiency with post-implantation embryonic progression and ionizing radiation sensitivity. Mutat Res 1998;409(1):17–29; doi: 10.1016/s0921-8777(98)00039-1

Mcneill DR, Whitaker AM, Stark WJ, et al. Functions of the major abasic endonuclease (APE1) in cell viability and genotoxin resistance. Mutagenesis 2020;35(1):27–38; doi: 10.1093/mutage/gez046

Meira LB, Devaraj S, Kisby GE, et al. Heterozygosity for the mouse Apex gene results in phenotypes associated with oxidative stress. Cancer Res 2001;61(14):5552–5557.

Mijit M, Caston R, Gampala S, et al. APE1/Ref-1—One target with multiple indications: Emerging aspects and new directions. J Cell Signal 2021;2(3):151–161.

Miyoshi H, Stappenbeck TS. In vitro expansion and genetic modification of gastrointestinal stem cells in spheroid culture. Nat Protoc 2013;8(12):2471–2482; doi: 10.1038/nprot.2013.153

Murata M, Thanan R, Ma N, et al. Role of nitrative and oxidative DNA damage in inflammation-related carcinogenesis. J Biomed Biotechnol 2012;2012:623019; doi: 10.1155/2012/623019

Murthy V, Tebaldi T, Yoshida T, et al. Hypomorphic mutation of the mouse Huntington's disease gene orthologue. PLoS Genet 2019;15(3):e1007765; doi: 10.1371/journal.pgen.1007765

Nakabeppu Y, Sekiguchi M. Physical association of pyrimidine dimer DNA glycosylase and apurinic/apyrimidinic DNA endonuclease essential for repair of ultraviolet-damaged DNA. Proc Natl Acad Sci U S A 1981;78(5):2742–2746; doi: 10.1073/pnas.78.5.2742

O'Hara AM, Bhattacharya A, Bai J, et al. Interleukin-8 induction by *Helicobacter pylori* in human gastric epithelial cells is dependent on apurinic/apyrimidinic endonuclease-1/redox factor-1. J Immunol 2006;177(11):7990–7999; doi: 10.4049/jimmunol.177.11.7990.

O'Hara AM, Bhattacharyya A, Bai J, et al. Tumor necrosis factor (TNF)-alpha-induced IL-8 expression in gastric epithelial cells: Role of reactive oxygen species and AP endonuclease-1/redox factor (Ref)-1. Cytokine 2009;46(3):359–369; doi: 10.1016/j.cyto.2009.03.010.

Ordway JM, Eberhart D, Curran T. Cysteine 64 of Ref-1 is not essential for redox regulation of AP-1 DNA binding. Mol Cell Biol 2003;23(12):4257–4266; doi: 10.1128/MCB.23.12.4257-4266.2003.

Raffoul JJ, Cabelof DC, Nakamura J, et al. Apurinic/apyrimidinic endonuclease (APE/REF-1) haploinsufficient mice display tissue-specific differences in DNA polymerase β-dependent base excision repair. J Biol Chem 2004;279(18):18425–18433; doi: 10.1074/jbc.M313983200

Ritchie ME, Phipson B, Wu D, et al. limma Powers differential expression analyses for RNA-sequencing and microarray studies. Nucleic Acids Res 2015;43(7):e47; doi: 10.1093/nar/gkv007

Robinson MD, Mccarthy DJ, Smyth GK. edgeR: A bioconductor package for differential expression analysis of digital gene expression data. Bioinformatics 2010;26(1):139–140; doi: 10.1093/bioinformatics/btp616

Rowe LA, Degtyareva N, Doetsch PW. DNA damage-induced reactive oxygen species (ROS) stress response in Saccharomyces cerevisiae. Free Radic Biol Med 2008;45(8):1167–1177; doi: 10.1016/j.freeradbiomed.2008.07.018

Santos JC, Funck A, Silva-Fernandes IJ, et al. Effect of APE1 T2197G (Asp148Glu) polymorphism on APE1, XRCC1, PARP1 and OGG1 expression in patients with colorectal cancer. Int J Mol Sci 2014;15(10):17333–17343; doi: 10.3390/ijms151017333

Schneider CA, Rasband WS, Eliceiri KW. NIH Image to ImageJ: 25 Years of image analysis. Nat Methods 2012;9(7):671–675; doi: 10.1038/nmeth.2089

Stavnezer J, Linehan EK, Thompson MR, et al. Differential expression of APE1 and APE2 in germinal centers promotes error-prone repair and A:T mutations during somatic hypermutation. Proc Natl Acad Sci U S A 2014;111(25):9217–9222; doi: 10.1073/pnas.1405590111

Stetler RA, Gao Y, Leak RK, et al. APE1/Ref-1 facilitates recovery of gray and white matter and neurological function after mild stroke injury. Proc Natl Acad Sci U S A 2016;113(25):E3558–E3567; doi: 10.1073/pnas.1606226113

Subramanian A, Tamayo P, Mootha VK, et al. Gene set enrichment analysis: A knowledge-based approach for interpreting genome-wide expression profiles. Proc Natl Acad Sci U S A 2005;102(43):15545; doi: 10.1073/pnas.0506580102

Suganya R, Chakraborty A, Miriyala S, et al. Suppression of oxidative phosphorylation in mouse embryonic fibroblast cells deficient in apurinic/apyrimidinic endonuclease. DNA Repair (Amst) 2015;27:40–48; doi: 10.1016/j.dnarep.2015.01.003

Unnikrishnan A, Raffoul JJ, Patel HV, et al. Oxidative stress alters base excision repair pathway and increases apoptotic response in apurinic/apyrimidinic endonuclease 1/redox factor-1 haploinsufficient mice. Free Radic Biol Med 2009;46(11):1488–1499; doi: 10.1016/j.freeradbiomed.2009.02.021

Vascotto C, Bisetto E, Li M, et al. Knock-in reconstitution studies reveal an unexpected role of Cys-65 in regulating APE1/Ref-1 subcellular trafficking and function. Mol Biol Cell 2011;22(20):3887–3901; doi: 10.1091/mbc.E11-05-0391

Xanthoudakis S, Miao GG, Curran T. The redox and DNA-repair activities of Ref-1 are encoded by nonoverlapping domains. Proc Natl Acad Sci U S A 1994;91(1):23–27; doi: 10.1073/pnas.91.1.23.

Xanthoudakis S, Smeyne RJ, Wallace JD, et al. The redox/DNA repair protein, Ref-1, is essential for early embryonic development in mice. Proc Natl Acad Sci U S A 1996;93(17): 8919–8923; doi: 10.1073/pnas.93.17.8919

Zou G-M, Luo M-H, Reed A, et al. Ape1 regulates hematopoietic differentiation of embryonic stem cells through its redox functional domain. Blood 2007;109(5):1917–1922; doi: 10.1182/blood-2006-08-044172

Address correspondence to:
Dr. Peter B. Ernst
Center of Veterinary Sciences and Comparative Medicine
Division of Comparative Pathology and Medicine
Department of Pathology
University of California, San Diego
La Jolla, CA
USA

E-mail: pernst@ucsd.edu

Date of first submission to ARS Central, July 19, 2021; date of final revised submission, June 6, 2022; date of acceptance, June 9, 2022.

Abbreviations Used

8-OHdG = 8-hydroxy-2-deoxyguanosine
γH2AX = phosphorylated H2AX
ANOVA = analysis of variance
APE1 = apurinic/apyrimidinic endonuclease 1
APEX1/Apex1 = gene name for APE1
BSA = bovine serum albumin
GO = Gene Ontology
Het = heterozygotic
HM = hypomorphic
KO = knockout
LA = long amplicon
MMS = methyl methanesulfonate
MRI = magnetic resonance imaging
mRNA = messenger RNA
mtDNA = mitochondrial DNA
MTT = 3-(4,5-dimethylthiazol-2-yl)-2,5-diphenyltetrazolium bromide
NeoR = neomycin resistance
PBS = phosphate buffered saline
PCR = polymerase chain reaction
RARE = rapid acquisition with relaxation enhancement
ROS = reactive oxygen species
Wt = wildtype